Available online at www.sciencedirect.com
SCIENCE DIRECT®
Chemical Physics 306 (2004) 171–183
Chemical Physics
www.elsevier.com/locate/chemphys

Absorption anisotropy studies of polymethine dyes

Richard S. Lepkowicz [a,*], Claudiu M. Cirloganu [a], Olga V. Przhonska [a,b], David J. Hagan [a,c], Eric W. Van Stryland [a], Mikhail V. Bondar [b], Yuriy L. Slominsky [d], Alexei D. Kachkovski [d], Elena I. Mayboroda [d]

[a] College of Optics and Photonics: CREOL & FPCE, University of Central Florida, Orlando, FL 32816-2700, USA
[b] Institute of Physics, National Academy of Sciences, Prospect Nauki 46, Kiev, 03028, Ukraine
[c] Physics department, University of Central Florida, Orlando, FL 32816-2700, USA
[d] Institute of Organic Chemistry, National Academy of Sciences, Murmanskaya 5, Kiev, 03094, Ukraine

Received 18 September 2003; accepted 22 July 2004
Available online 14 August 2004

Abstract

The determination of the spectral position of the excited states and orientation of the transition dipole moments of polymethine molecules is experimentally measured using two methods: the steady-state fluorescence anisotropy method, and a two-color polarization-resolved pump–probe method. This novel use of the pump–probe method is described in detail and a comparison to the fluorescence method is given. Quantum-chemical modeling on the effects of the bridge structure in the polymethine chromophore on the linear absorption spectrum is also discussed.

Keywords: Exited-state absorption; Polymethine dye; Orientation of transition dipole moments; Anisotropy; Pump–probe

1. Introduction

Polymethine dyes (PDs) are promising compounds for nonlinear optical applications, such as optical limiting, due to a strong and broad excited-state absorption (ESA) in the visible region. Our efforts have been directed toward a systematic study of the spectroscopic and nonlinear optical properties of a series of PDs in various host environments [1–4]. It is relatively easy to modify the PDs structure using different heterocyclic terminal groups, different lengths of the polymethine chain, and introduction of specific substitutes into the polymethine chain and cyclization of the chain by conjugated or unconjugated bridges. These studies led to the development of PDs with ESA cross-sections as large as 7×10^{-16} cm^2, which is comparable to that of the ground state at its peak [1,2]. A detailed investigation of the ESA dynamics and molecular motions in liquid solutions and in an elastic polymeric media using a time-resolved induced anisotropy method has been performed [3,4]. However, a comparison of these results with steady-state fluorescence anisotropy spectroscopy left some questions unanswered.

In this paper, we describe experimental studies and give an analysis of the spectral position and the orientation of the transition dipole moments connected with the $S_0 \rightarrow S_n$ transitions ($n = 1, 2, 3, \ldots$) in a set of polymethine molecules. The orientation of the $S_0 \rightarrow S_n$ transition dipole moments are commonly determined relative to the fluorescence transition dipole moment ($S_1 \rightarrow S_0$) using the fluorescence anisotropy method. We demonstrate for the first time that the pump–probe

* Corresponding author. Present address: Optical science division, Naval Research Lab, 4555 Overlook Ave SW, 203755338 Washington, USA. Tel.: +1 2024043662/+1 407 823 6865; fax: +1 2024048114/+1 407 823 6880.
E-mail addresses: rlepkowi@mail.ucf.edu, lepkowicz@sisyphus.nrl.navy.mil (R.S. Lepkowicz).

0301-0104/$ - see front matter © 2004 Elsevier B.V. All rights reserved.
doi:10.1016/j.chemphys.2004.07.021

technique, which probes the orientation of the ESA transition dipole moments $S_1 \rightarrow S_n$ ($n = 2, 3, 4,\ldots$), can be used to determine the spectral position and orientation of the transition dipole moments connected with the $S_0 \rightarrow S_n$ transitions ($n = 1, 2, 3,\ldots$). We show for the essentially linear polymethine molecules that the ESA transition moments can be used for determining the orientation of the $S_0 \rightarrow S_n$ transitions instead of the fluorescence transition dipole moment ($S_1 \rightarrow S_0$). This important conclusion relies on the fact that the transition dipole moment of the most intensive $S_0 \rightarrow S_1$ absorption band, which is known to be parallel to the direction of the polymethine chain (or molecular backbone), is much larger (20–400 times) than for all higher transitions ($S_0 \rightarrow S_n$, $n > 1$). Based on these results we propose a new approach for the investigation of the anisotropy properties of linear polymethine molecules, which can be applied to cases in which the steady-state measurements cannot be used, e.g., in cases of nonfluorescent molecules (e.g., IR-dyes) or solvents with low viscosity which decreases the anisotropy value due to reorientational diffusion.

The experimental techniques used to investigate the PD molecules are:

1. Linear absorption spectral measurements.
2. Steady-state excitation fluorescence anisotropy measurements.
3. Two-color picosecond polarization-resolved pump–probe measurements.

The analysis includes:

1. Quantum-chemical calculations.
2. Numerical fitting of the pump–probe measurements.

2. Materials

The molecular structures of the polymethine dyes studied are shown in Fig. 1. Their chemical names are: 3,3,3,3-tetramethyl-1,1-diphenylindotricarbocyanine perchlorate (labeled as PD 3428); 2-[2-[3-[(1,3-dihydro-1,3,3-trimethyl-5-phenyl-2H-indol-2-ylidene)ethylidene]-2-phenyl-1-cyclohexen-1-yl]ethenyl]-1,3,3-trimethyl-5-phenylindolium tetrafluoroborate (labeled as PD 2338); 1,3,3-trimethyl-2-(2-{2-phenyl-3[2-(1,3,3-trimethyl-1,3-dihydroindo-2-ylidene)ethylidene]cyclopent-1-enyl}vinyl)-3H-indolium tetrafluoroborate(labeled as PD 1952); 1,3,3-trimethyl-2-(2-{2-phenyl-3[2-(1,3,3-trimethyl-1,3-dihydroindo-2-ylidene)ethylidene]cyclopenta-1,4-dienyl}vinyl)-3H-indolium perchlorate (labeled as PD 2410); 2-[9-(1-ethyl-3,3-dimethyl-2H-benzo[e]indol-2-ylidene)-3,7-dimethyl-4,6-(2,2-dimethyltrimethylene)-1,3,5,7-nonatetraenyl]-1-ethyl-3,3-dimethylbenzo[e]indolium perchlorate (labeled as PD 2332). These PDs were synthesized at the Institute of Organic Chemistry, Kiev, Ukraine. Their molecular

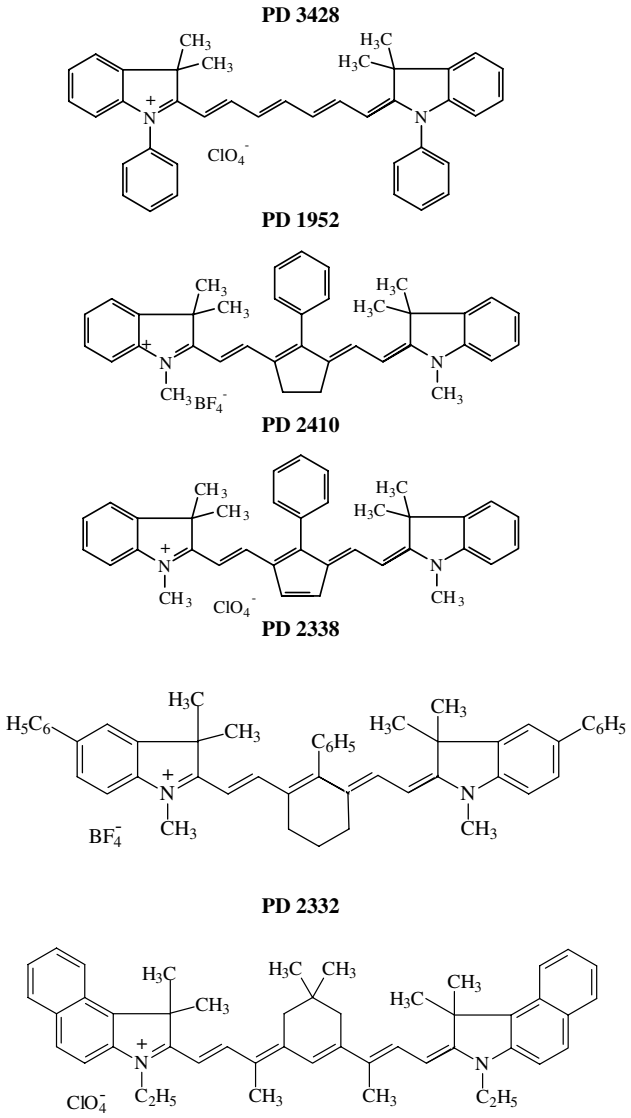

Fig. 1. Molecular structures of PDs.

structures were confirmed by elemental analysis and nuclear magnetic resonance spectra measurements. Synthesis of PDs 2350 and 3428 is performed by standard methods described in [5]. Specific synthesis for the dyes with bridged polymethine chromophores (PDs 1952, 2410, 2338 and 2332) is described in [6]. The linear absorption spectra of the dyes in ethanol, presented in Fig. 2, were recorded with a Varian Cary 500 spectrophotometer.

The spectroscopic properties of PDs are determined by the existence of a delocalized π-electron system in the polymethine chromophore (or polymethine chain) and symmetric terminal groups of a similar nature (indolenine residues). The dyes PD 3428, 2338, 1952 and 2410 all have the same length of the polymethine chain (tricarbocyanines). PD 3428 is unique in the fact that it has an unsubstituted (or unbridged) polymethine chromophore. Other tricarbocyanines differ by the nature of the bridge group: six-membered cycle (or trimeth-

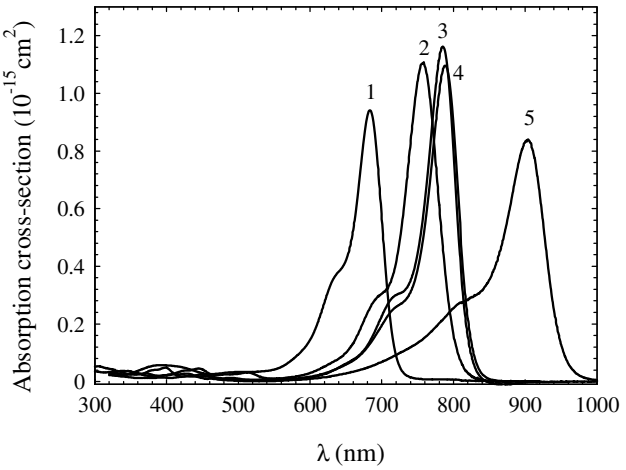

Fig. 2. Linear absorption spectra for: PD 2410 (1), PD 3428 (2), PD 2338 (3), PD 1952 (4), PD 2332 (5) in ethanol.

ylene bridge) for PD 2338, five-membered cycle (or dimethylene bridge) for PD 1952 and five-membered cycle with an extra double bond (or vinylene bridge) for PD 2410. Therefore, using this series of dyes, we can study the effect of the bridge group on their spectroscopic and anisotropy properties. The absorption maxima for PDs 2338 and 1952 are shifted into the red region to 784 and 788 nm relative to the unsubstituted PD 3428 (757 nm). PD 2338 is characterized as having the largest (within the tricarbocyanines) ground-state absorption cross-section ($\sigma_g = 1.2 \times 10^{-15}$ cm^{-2}). The absorption maximum for PD 2410 is blue shifted to 684 nm due to the influence of the negatively charged vinylene bridge group. The effect of the bridge group on the position of the absorption band is explained in more detail in Section 5. For the tetracarbocyanine PD 2332, $\sigma_g = 0.8 \times 10^{-15}$ cm^{-2}. PD 2332 is the longest polymethine chain dye included in this study, and has the longest π-electron system in the terminal groups, which explains the long wavelength spectral position with the maximum at 904 nm. PD 2332 was chosen particularly for the anisotropy studies.

3. Experimental methods

3.1. Steady-state fluorescence excitation anisotropy measurements

Steady-state fluorescence spectra (using low concentrated, 10^{-6} M, to avoid reabsorption) and excitation anisotropy spectra were obtained with a PTI Quantamaster Spectrofluorimeter. All measurements were conducted in high viscosity glycerol solutions in which the rate of reorientation ($\tau_R \approx 200$ ns) is much slower than the excited-state lifetime ($\tau_F \approx 1$ ns), thus the effects of rotational diffusion on the anisotropy integrated over the lifetime of the sample are negligible ($\leqslant 0.5\%$). Excitation anisotropy measurements give us information about the spectral position and orientation of the transition dipole moments from the ground to first and higher excited states $S_0 \rightarrow S_n$ ($n = 1, 2, 3,\ldots$) relative to the fluorescence transition dipole moment ($S_1 \rightarrow S_0$) [7]. The excitation anisotropy spectrum, $R(\lambda)$, is calculated as a function of the excitation wavelength λ at a fixed emission wavelength (usually near the fluorescence maximum) after appropriate background subtraction on each component:

$$R(\lambda) = \frac{I_{vv}(\lambda) - G(\lambda) I_{vh}(\lambda)}{I_{vv}(\lambda) + 2G(\lambda) I_{vh}(\lambda)}, \tag{1}$$

where $G(\lambda) = I_{hv}(\lambda)/I_{hh}(\lambda)$ and $I_{vv}(\lambda)$, $I_{hv}(\lambda)$, $I_{vh}(\lambda)$, $I_{hh}(\lambda)$ are the polarized fluorescence intensities at the excitation wavelength [7]. The first and second subscripts refer to the orientation (v for vertical and h for horizontal) of the excitation and emission polarizations, respectively. The angle between the absorption and emission transition moments can be determined from the anisotropy $R(\lambda)$ by:

$$R = \frac{2}{5}\left(\frac{3\cos^2(\beta) - 1}{2}\right), \tag{2}$$

where β is the angle between the absorption transition dipole moment and the emission transition dipole moment [7]. The results of the steady-state fluorescence excitation anisotropy measurements are presented below.

3.2. Two-color picosecond polarization-resolved pump–probe measurements

The laser system used for these experiments is a 10-Hz *EKSPLA* PL2143 Nd:YAG laser and an *EKSPLA* PG401/DFG optical parametric generator (OPG) tunable from 0.42 to 2.3 μm. The second harmonic (532 nm) of the Nd:YAG laser with a pulse width of 24 ps (FWHM) is used as the probe. The pump is the output of the OPG over the range of 420–900 nm. The basic experimental set-up is shown in Fig. 3. The energy range of the pump beam is between 2 and 20 μJ, while the probe is held to approximately 1 nJ. The probe beam is focused to a waist of 30 μm (half width $1/e^2$ maximum), while the pump beam's focused waist changes size based on wavelength from 120 to 250 μm (half width $1/e^2$ maximum) over the range of 420–900 nm, respectively. The pump beam is much larger than the probe beam to ensure that the probe beam senses a uniform excitation region in the sample. The pump irradiance is at least forty times larger than that of the probe and in most cases several hundred times larger.

The probe beam can be temporally delayed with respect to the pump beam up to 15 ns, but for the determination of the peak anisotropy only short scans of 10 ps

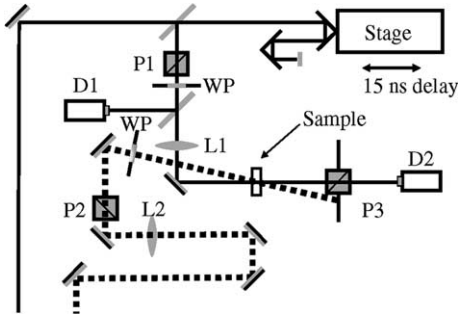

Fig. 3. Schematic of pump–prope setup. Probe beam is represented as solid line and pump beam is represented as dotted line. P1,2,3: polarizers, D1,2: detectors, L1,2: lenses, WP: half-wave plate.

were performed. The reason for determining the anisotropy in the first 5–10 ps after excitation is to avoid reorientational diffusion effects in the lower viscosity ethanol solutions used in the pump–probe experiment. The rate of reorientation ($\tau_R \approx 300$–400 ps [4]) of the polymethines in ethanol is typically less than the excited-state lifetime ($\tau_F \approx 1$ ns), but by taking the anisotropy as the average value over the first 5–10 ps there is no need to correct for orientational diffusion effects or to average it over the fluorescence lifetime. The pump and the probe beams are overlapped at a small angle (~5°) within the sample so the probe beam can be separated after the sample from the pump as shown in Fig. 3. The polarization of the probe is fixed and a polarizer placed after the sample is aligned parallel with the probe polarization. The pump polarization is adjusted with a half-wave plate and can be set to any angle with respect to the probe polarization. The probe beam is monitored before and after the sample using large area silicon photodiodes (1 cm diameter).

4. Results

4.1. Steady-state fluorescence excitation anisotropy data

It is well known that the absorption spectra in the visible and near IR region for PDs are characterized by a strong single band, corresponding to the $S_0 \rightarrow S_1$ transition, with a typical FWHM = (750–950) cm^{-1} – see Fig. 2. A small vibration maximum due to carbon–carbon skeleton vibrations is situated about 1200 cm^{-1} above the main absorption peak. The absorption spectrum in the short wavelength region is characterized by small intensity and strongly overlapped bands, which correspond to the $S_0 \rightarrow S_n$ ($n = 2, 3, \ldots$) transitions. The excitation anisotropy measurements reveal the spectral position of these transitions and the angles between the absorption and fluorescence transition dipole moments. In these measurements, the fluorescence intensity near the peak position, resolved into parallel ($I_{||}$) and perpendicular ($I_{\perp}$) components relative to the excitation polarization, is measured as a function of excitation wavelength (λ). The steady-state anisotropy excitation spectra, $R(\lambda)$, for PDs 3428, 2338, 1952 and 2410 are presented in Fig. 4. For some dyes the anisotropy values are close to the theoretical limit of 0.4 [7], showing that the orientation of the absorption and emission transition dipole moments are parallel. Measurements were also performed in ethanol to check if any spectral shift in the position of the excited states occurs in different solvents. No shifts are observed, but the maximum value of anisotropy, without correcting for the reorientational diffusion effects, decreases to 0.06–0.07. The steady-state anisotropy excitation spectra, $R(\lambda)$, were measured within the whole absorption spectrum, including peak position and vibronic region. No changes in anisotropy value due to vibrational coupling were observed.

From the experimental results presented in Fig. 4, we can locate the positions of the $S_0 \rightarrow S_n$ transitions. For all dyes the highest anisotropy values are observed for the $S_0 \rightarrow S_1$ transition: 0.3 for PD 1952, 0.32 for PD 2338, 0.34 for PD 3428 and 0.38 for PD 2410. The smallest (negative values) are observed for PD 1952 for the $S_0 \rightarrow S_2$ transition and in PD 2338 for the $S_0 \rightarrow S_4$ transition. PD 2410 shows an unusual behavior in the anisotropy within several of the $S_0 \rightarrow S_n$ bands, which will be discussed in more detail in Section 5. The positions of the $S_0 \rightarrow S_n$ transitions revealed from the anisotropy spectra, $R(\lambda)$, show good correlation with the positions of the short wavelength absorption bands for all dyes (see also analysis in [4]).

4.2. Two-color picosecond polarization-resolved pump–probe data

The pump–probe method has been used by several groups (for example [8,9]) to measure the orientation of the excited-state transition dipole moments. We are proposing to use the orientation of an ESA transition dipole moment to measure the spectral location and orientation of the ground-state transitions ($S_0 \rightarrow S_n$) relative to the fluorescence transition ($S_1 \rightarrow S_0$). The method of computing the anisotropy from the pump–probe experiment is explained in detail in Ref. [4]. The main point is the change in transmission of the probe for polarizations parallel ($\Delta T_{||}$) and perpendicular ($\Delta T_{\perp}$) to that of the pump polarization replace I_{vv}, I_{vh} in Eq. (1). In the case of the pump–probe experiment the angle β in Eq. (2) refers to the angle between the absorption transition dipole moment of the pump and the absorption transition dipole moment of the probe. The $S_1 \rightarrow S_5$ transition has been shown [1–4] to be connected with the most intense excited-state transition and the probe wavelength of 532 nm is close to the peak of the ESA spectrum. This point is more thoroughly covered in Section 5.4.

Figs. 4(b)–(d) shows the anisotropy spectra for PDs 2338, 1952 and 2410, calculated from the pump–probe

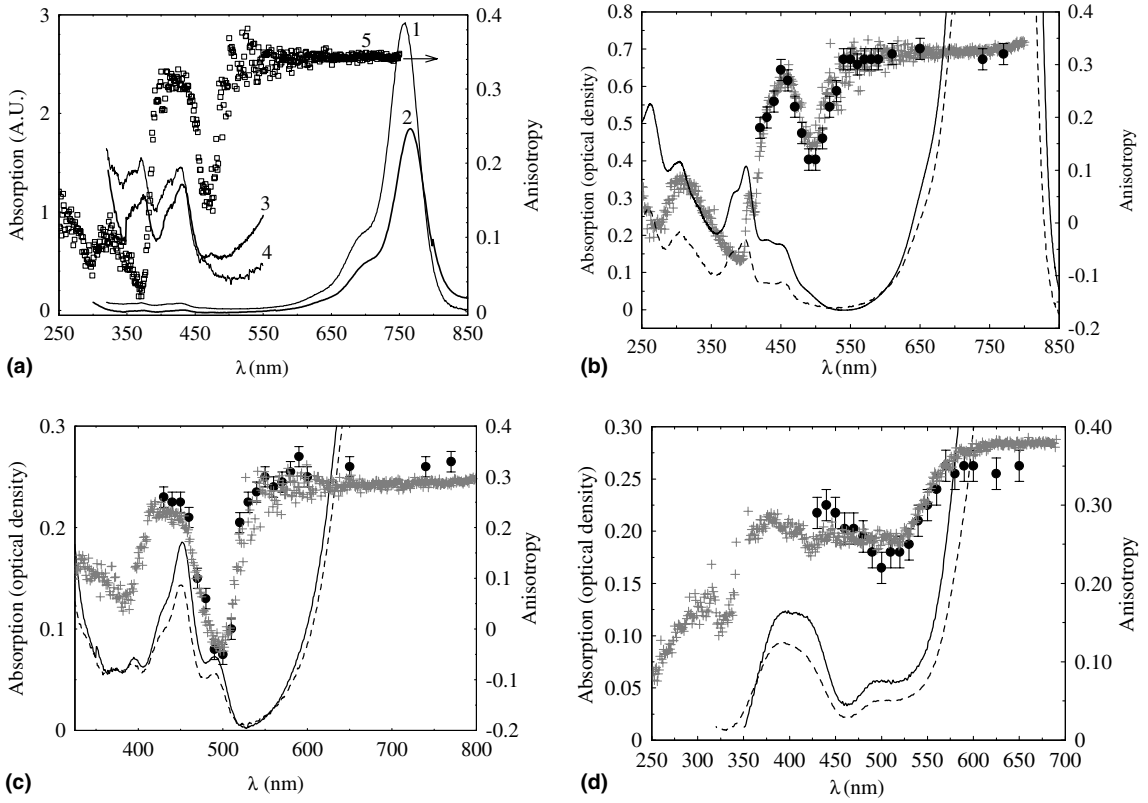

Fig. 4. (a) Linear absorption (A.U.) (left axis) and steady-state anisotropy (right axis) for PD 3428 in ethanol and glycerol. Linear absorption in: (1) ethanol, (2) glycerol, (3) and (4) are higher concentration samples of ethanol and glycerol, respectively, to show details of the spectral location of excited states, (5) steady-state anisotropy in glycerol. For PDs 2338 (b) 1952 (c) and 2410 (d) is shown the steady-state (+) and ESA (●) anisotropy (right axis) along with linear absorption (optical density) (left axis) in ethanol (dotted line) and glycerol (solid line).

experiments with the tunable pump from 420 to 900 nm, along with the anisotropy curves measured using the steady-state fluorescence method. There is very good correlation between these two methods. Both pump–probe and fluorescence methods can resolve all the features in the anisotropy data for the tricarbocyanine dyes; however, the pump–probe method has the distinct advantage of being applicable to a wider range of molecules (i.e., nonfluorescent molecules). On the other hand, the pump–probe experiment takes considerably more time to perform and requires short-pulsed tunable sources.

We applied this method to study the anisotropy of the tetracarbocyanine dye PD 2332. Because of its long wavelength spectral position, the fluorescence quantum yield is very small and we could not perform the steady-state fluorescence measurements using the existing PTI Quantamaster Spectrofluorimeter. Pump–probe anisotropy results for this dye are shown in Fig. 5 along with its absorption spectrum in this region. The following four electron transitions could be resolved from this data. As can be seen, the anisotropy values are relatively high (≈0.3) and constant over the $S_0 \rightarrow S_1$ transition and exhibit a significant drop (to 0.13) over the second band ($S_0 \rightarrow S_2$ transition) with the peak position around 570 nm. The next increase in the anisotropy value reveals the position of the $S_0 \rightarrow S_3$ transition (470–520 nm), which is nearly parallel to the $S_0 \rightarrow S_1$ transition dipole moment. The next drop in anisotropy (to 0) corresponds to the position of the $S_0 \rightarrow S_4$ transition (near 450 nm) and indicates a significant angle relative to the $S_0 \rightarrow S_1$ transition dipole moment.

From our point of view, ESA anisotropy measurements represent a very useful approach which can be applied to cases in which the steady-state method cannot

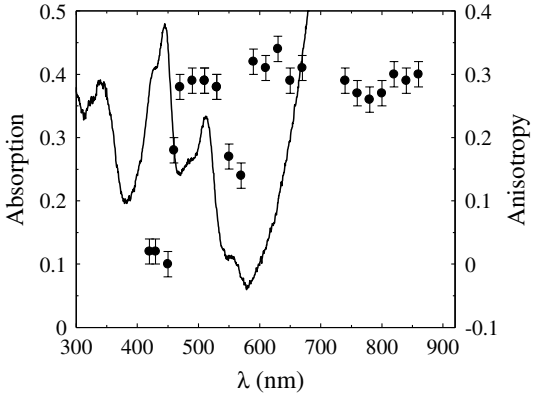

Fig. 5. ESA anisotropy (right) for PD 2332 along with linear absorption (optical density) (left) in ethanol.

be used, for example in cases of nonfluorescent (or low fluorescence quantum yield) molecules or solvents with low viscosity which decreases the anisotropy value due to reorientational diffusion.

5. Discussion

5.1. Methodology of quantum-chemical calculations

The equilibrium molecular geometry and the electron charge distribution for the dyes in the ground and excited states were performed employing the semi empirical AM1 method (MOPAC package, gradient <0.01 kcal/mol). It was demonstrated previously that the charges and C—C bond lengths calculated in this method are in good agreement with the corresponding values obtained in the ab initio approximation [10,11]. The optimization of the geometry in the excited state was calculated taking into account the changes in the bond lengths and valence angles (optimization of the torsion angles is not considered). This approximation is valid since the steady-state anisotropy measurements were performed in a highly viscous glycerol solution preventing significant torsion deformations, and the ESA anisotropy experiments were measured in the first 5–10 ps before large changes in the torsion angles could occur. See details below. The wave function of the excited state is expressed as the expansion of the excited configurations corresponding to all the possible electron transitions from the three highest occupied molecular orbitals (HOMO) and to the two lowest unoccupied molecular orbitals (LUMO).

5.2. Quantum-chemical calculation: molecular geometry and electron density distribution

Quantum-chemical calculations were performed with the goal of understanding the features of the electron density distribution in the ground and excited states as well as the changes in the molecular geometry of PDs under excitation. The principle photophysical properties of the polymethine dyes are determined by the electronic structure of the conjugated chain. In turn, the features of the electronic structure of the polymethine chain in the ground and excited states is due to the existence of the charges of the π-electron system. It has been established that the total charge, both positive and negative in conjugated molecular ions, induces the partial charges at the π-centers [11–13]. As an example, Fig. 6(a) presents the ground state charge distribution at the carbon atoms in the model chromophore.

$$H_2C^+–(CH{=}CH)_{10}–CH{=}CH_2 \quad (3)$$

It is seen from Fig. 6(a) that there is considerable alternation of the charge magnitudes at the neighboring atoms. The amplitude of the alternation increases regularly from the end of the chain to the middle of the chain. This wave is similar to the charge wave of finite length due to the doping of an electron or a hole into the neutral π-conjugated system of polymers (such as polyacetylene) and is directly connected with the alternation of the lengths of the neighboring C–C bonds [10,11]. This length alternation for the model chromophore (3) is presented in Fig. 6(b). It has been proposed that the meaningful quantity is the difference in bond lengths between neighboring C–C bonds, which is given by the bond length alternation as $\Delta l = |l_{n,\,n+1} - l_{n+1,\,n+2}|$, where $l_{n,\,n+1}$ is the bond length between two neighboring n and $n+1$ carbon atoms (π-centers) [10,14]. Similarly, the differential property of the charge wave can be described by the amplitude of charge alternation, $\Delta q = |q_n - q_{n+1}|$, where q_n and q_{n+1} are the charges at two neighboring n and $n+1$ atoms [11,15,16]. The maximum of the Δq-function corresponds to the middle of the conjugated chain. The minimum of the Δl-function coincides with the maximum of

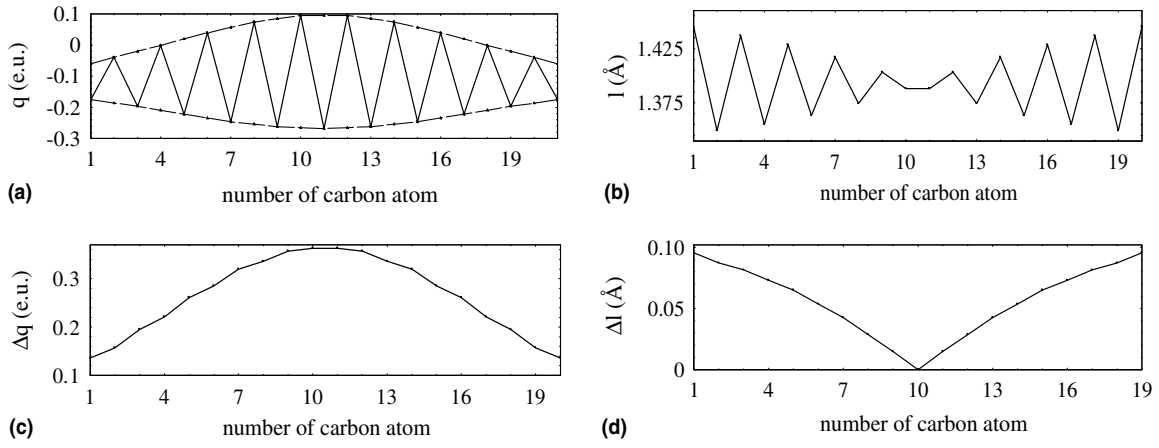

Fig. 6. (a) Charge distribution at the carbon atoms, (b) carbon–carbon bond lengths, (c) charge alternation, and (d) bond length alternation in the ground state for the model chromophore $H_2C^+–(CH{=}CH)_{10}CH{=}CH_2$.

the charge wave. This is a general rule for an arbitrary molecule in the global energy minimum in the ground state [15,16]. Both ground state Δq- and Δl-functions for the model chromophore (3) are presented in Figs. 6(c) and (d).

Introduction of the terminal groups and the cycle bridges into the structure of the model chromophore leads to a shape distortion of both the charge and the length amplitude alternation functions. Below we give a detailed analysis of the charge density distribution and optimal geometries in the ground and excited states for the tricarbocyanine PDs 3428, 2338, 1952, 2410 and the tetracarbocyanine PD 2332.

5.2.1. PD 3428

The dependence of the amplitude of the charge alternation, Δq, and the bond length alternation, Δl, for the main part of the polymethine chromophore (between nitrogen atoms in indolenine terminal groups) for unsubstituted PD 3428 is presented in Figs. 7(a) and (b). Comparison with Figs. 6(c) and (d) shows that the end groups cause a deformation in the shape of the Δq-wave: with an increase in the amplitude near the nitrogen atoms of the terminal groups and nearly the same values at the middle of the chain. The amplitude of the charge wave becomes nearly flat throughout the polymethine chain. The shape of the Δl-function remains unchanged with the minimum at the middle of the chain and a very small bond alternation in the ground

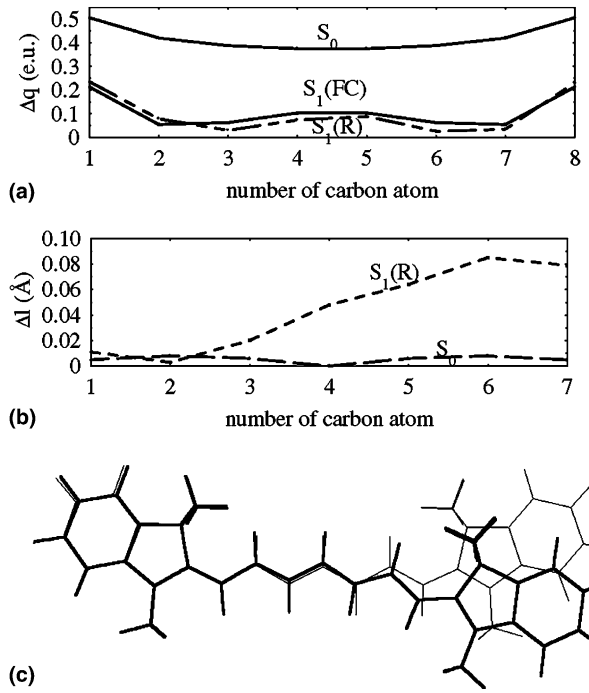

Fig. 7. (a) Charge alternation in the ground and excited state, (b) bond length alternation in the ground and relaxed excited state, and (c) optimized geometries in the ground (grey structure) and excited (black structure) state for PD 3428.

state (≈10 times less than the model chromophore). Immediately after the $S_0 \rightarrow S_1$ transition the charge distribution will be changed. Fig. 7(a) presents the charge distribution in the first excited state for two geometries: the Franck–Condon geometry (FC) corresponding to the ground-state unaltered geometry, and the so called relaxed geometry (R), which could be obtained as a result of vibronic relaxation in the excited state causing changes in the valence angles and bond lengths. It is easily seen that the excitation leads to a considerable decrease in charge alternation. Also, the charge wave exhibits two degenerate minima, which become more pronounced and asymmetric in the relaxed geometry, but in general there are no substantial changes between Δq-functions in the FC or R S_1-state. The calculated bond length changes due to vibrational relaxation are considerable and are presented in Fig. 7(b). The optimized geometries in the ground and excited-state are drawn in Fig. 7(c). It should be mentioned that for simplicity we considered a dye structure with methyl substitutes near the nitrogen atoms instead of the phenyl groups for the geometry optimization. These changes do not affect the main characteristics discussed. In Fig. 7(b), it can be seen that the Δl at the first carbon atom of the chain (near one of the terminal groups) is nearly the same in the S_1 relaxed state and the S_0 ground state. We take advantage of this fact to compare the optimized geometries of the ground and excited-state configuration by overlapping the two configurations at this point. From Fig. 7(c), it is clearly seen that the deviation of the N–N axis is about 20° due to geometric relaxation. From our point of view, these changes in geometry are responsible for the anisotropy value of the $S_0 \rightarrow S_1$ transition. A decrease in anisotropy from the theoretical value over the spectral range of the $S_0 \rightarrow S_1$ transition of 0.4 to the observed value of 0.34 is in good agreement with a deviation of the N–N axis of approximately 20°.

5.2.2. PD 2338

The dependence of the amplitude of the charge alternation, Δq, and the bond length alternation, Δl, for PD 2338 in the ground and the first excited state, S_1, are presented in Figs. 8(a) and (b). Cyclization of the part of the polymethine chromophore by a six-membered cycle (trimethylene bridge) with a phenyl substitute in the mesoposition of the chromophore situated perpendicular to the molecular plane, does not cause a considerable distortion of the ground-state Δq- and Δl-functions with respect to the unsubstituted PD 3428. However, the two degenerate minima of the charge wave in the S_1-state become more pronounced and exhibit an asymmetric behavior in the relaxed geometry. The amplitude of the bond alternation becomes asymmetric as well. The trimethylene bridge keeps the minimum of the Δl-function at the middle of the chain but allows an asymmetric increase in the amplitudes at the beginning and the end

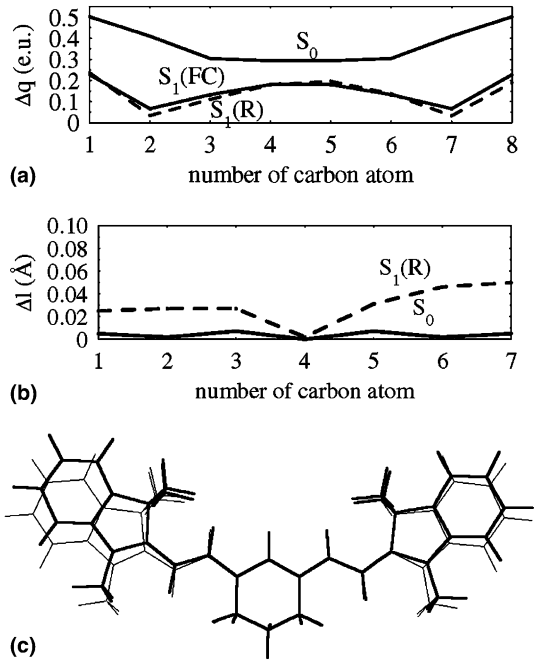

Fig. 8. (a) Charge alternation in the ground and excited state, (b) bond length alternation in the ground and relaxed excited state, and (c) optimized geometries in the ground (grey structure) and excited (black structure) state for PD 2338.

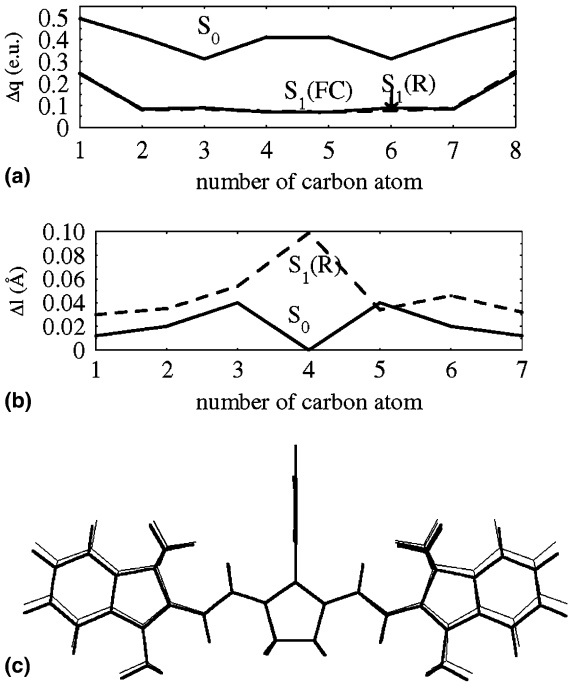

Fig. 9. (a) Charge alternation in the ground and excited state, (b) bond length alternation in the ground and relaxed excited state, and (c) optimized geometries in the ground (grey structure) and excited (black structure) state for PD 1952.

of the chain. Both optimized geometries in the ground and excited state are shown in Fig. 8(c). For simplicity in the optimization of the geometry, we neglected the two phenyl substitutes in the terminal groups (which do not affect the main properties) and considered the simpler analog of PD 2338. For this dye, the minimum bond length distortion in the S_1 state is observed near the center of the chromophore. Therefore, following the same logic as for PD 3428, we combined both optimized geometries over the central position of the chain. From Fig. 8(c), it can be seen that the distortion of the chromophore (and N–N axis) becomes more complicated and leads to two different bending angles for the two parts of the chain separated by the bridge group of about 10° and 6°, respectively. Therefore, it is difficult to perform a direct comparison between the angles of rotation of the N–N-axis and the anisotropy of the $S_0 \rightarrow S_1$ transition. In any case, the total angle does not exceed 20°, which could explain the observed anisotropy value over the $S_0 \rightarrow S_1$ transition of 0.32.

5.2.3. PD 1952

The electron structure and equilibrium geometry of the polymethine chain in PD 1952, presented in Figs. 9(a) and (b), are much more sensitive to cyclization by the five-membered cycle (dimethylene bridge) as compare to that of cyclization by the six-membered bridge. First of all, the dimethylene bridge leads to bending of the chain even in the ground state, so that the angle between the line connecting the two nitrogen atoms (N–N axis) and the line connecting one of these nitrogen atoms with the carbon atom in the mesoposition of the chain is about 15° (the corresponding value for unsubstituted PD 3428 is only 7°). In the excited state the difference in the length of the two central C–C bonds increases considerably leading to a symmetry breaking in the equilibrium molecular geometry, as seen in Fig. 9(b). Secondly, the amplitude of the charge wave in the ground state shows two minima due to a strong influence of the dimethylene bridge; on the other hand, the excited-state relaxation does not cause any substantial changes in the electron charge distribution.

Optimized ground and excited-state geometries for PD 1952 are shown in Fig. 9(c). For this dye, the minimum bond length distortion in the excited state is observed near the 5th carbon atom of the chromophore. Therefore, following the same logic as with the previous dyes, we combined both optimized geometries over this position. As can be seen in Fig. 9(c) there is only a slight additional deformation of the chromophore in the excited state. For this dye it is difficult to perform a direct comparison with the anisotropy of the $S_0 \rightarrow S_1$ transition. Probably, the strong bending of the polymethine chromophore is responsible for the observed anisotropy value over the $S_0 \rightarrow S_1$ transition of 0.3.

5.2.4. PD 2410

Considerable changes in the alternation of both charge and geometrical characteristics are observed for PD 2410 that has a five-membered vinylene bridge conjugated with the main π-electron system of the chain. Figs. 10(a)–(c) represent all calculated quantum-chemical parameters. As can be seen, the vinylene bridge causes a substantial bond length distortion in the ground state, but this distortion remains nearly constant in the excited state in contrast to that of PD 1952. Overlapping both of the molecular geometries with respect to the central bond, we observe the smallest change in the orientation of the polymethine chromophore, which probably explains the high anisotropy value of 0.38, which was observed experimentally. It is interesting to note that such cyclization leads to considerable symmetry breaking in the charge distribution after the geometrical relaxation as seen in Fig. 10(a).

5.2.5. PD 2332

The indotetracarbocyanine, PD 2332, differs from the other dyes by an increased length of the conjugated π-electron system. The ground-state Δq-function shows two degenerate minima, which become asymmetric in the S_1-state after the geometrical relaxation (Fig. 11(a)). The behavior of the Δl-function for this dye (Fig. 11(b)) shows some similarity with the Δl-function of the unsubstituted PD 3428. Overlap of both of the optimized molecular geometries, ground state and relaxed state, with respect to the bond with the minimum difference of Δl between the ground and relaxed state is shown in Fig. 11(c).

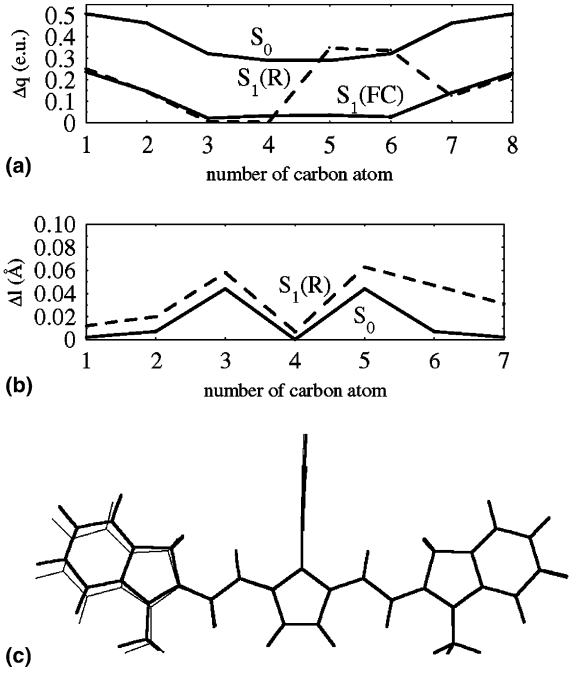

Fig. 10. (a) Charge alternation in the ground and excited state, (b) bond length alternation in the ground and relaxed excited state, and (c) optimized geometries in the ground (grey structure) and excited (black structure) state for PD 2410.

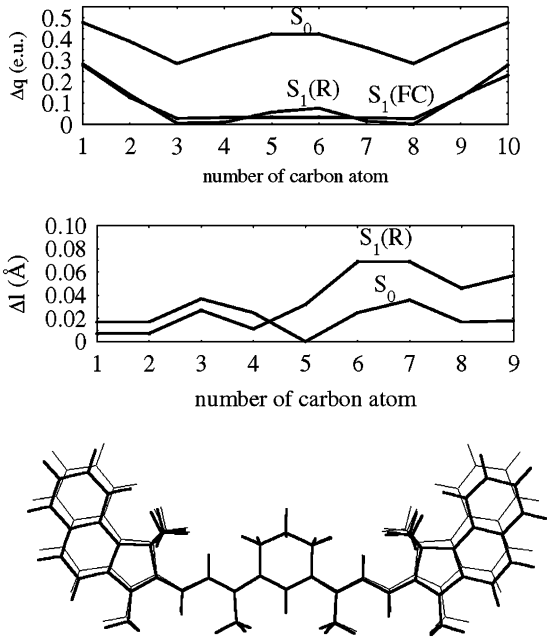

Fig. 11. (a) Charge alternation in the ground and excited state, (b) bond length alternation in the ground and relaxed excited state, and (c) optimized geometries in the ground (grey structure) and excited (black structure) state for PD 2332.

Quantum-chemical analysis of the charge distribution and optimal geometries for the PDs under study leads to the following conclusions:

1. All features of the electron density distribution and molecular geometry in the ground and first excited state, S_1, can be explained using the two functions of amplitude of the charge alternation (Δq) and bond length alternation (Δl).
2. Introduction of the terminal groups to the model polymethine chromophore causes a deformation in the shape of the charge wave leading to an increase of the amplitude near the nitrogen atoms of these terminal groups.
3. The $S_0 \rightarrow S_1$ excitation leads to a considerable decrease in the amplitude of the charge alternation. Also in the S_1-state the charge wave exhibits two degenerate minima, which become more pronounced and asymmetric in the relaxed geometry.
4. Cyclization of the part of the polymethine chromophore by a six-membered cycle (trimethylene bridge) does not cause considerable distortion of the ground-state Δq- and Δl-functions with respect to the unsubstituted chromophore. The distortion of the equilibrium geometry of the polymethine chain in PDs due to a five-membered cycle (dimethylene

bridge) is substantial. This distortion occurs even in the ground state of the molecule which leads to an increase in the ground state absorption cross-section.

5. Deformations in the molecular geometry under excitation (from Franck–Condon to relaxed state), accompanied by changes in the valence angles and bond lengths, are responsible for the change in anisotropy over the $S_0 \rightarrow S_1$ transition from the theoretical value of 0.4 to the experimentally measured values of 0.30–0.38 (depending on the dye) for the $S_0 \rightarrow S_1$ transition.

5.3. Quantum-chemical calculation: electron transitions and effect of the cyclization by hydrocarbon bridge group

5.3.1. Charge redistribution under the excitation

The excitation of the dye molecule by light and hence the promotion of an electron from one of the HOMO to one of the LUMO is accompanied by a substantial redistribution of the charges on the atoms. It was established that under excitation the electron densities at the carbon atoms in the odd positions of the polymethine chain decrease while those at the even positions increase [12,13,17]. Thus, there is a considerable difference in the changes of the charge at the neighboring atoms in the chain. Similarly the amplitudes of the charge and bond length alternation functions (Δq and Δl), under excitation can be characterized by the amplitude $Q = |\Delta q^* - \Delta q^0|$, where Δq^0 and Δq^* are Δq-functions in the ground and excited S_1-states, respectively. These functions for PDs 3428, 2338, 1952 and 2410 are presented in Fig. 12(a). We can note that the maximum of the electron density redistribution always corresponds to the center of the polymethine chromophore for all dyes independently of the bridge type. Amplitudes of PDs 3428, 2338, 1952 are approximately equal and the amplitude of charge redistribution for PD 2410 is much less. This trend corresponds to their absorption cross-sections presented in Fig. 2.

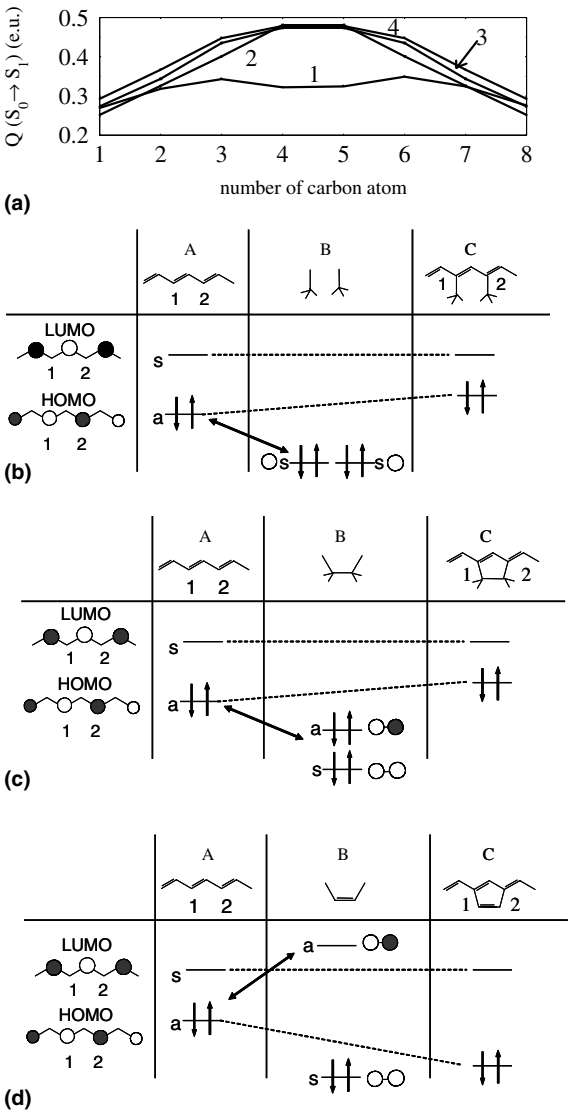

Fig. 12. (a)Electron density redistribution for the $S_0 \rightarrow S_1$ transition for PD 2410 (1), PD 1952 (2), PD 2338 (3), and PD 3428 (4). The effects of the bridges on the energy levels for PD 2338 (b), PD 1952 (c) and PD 2410 (d). Where (A) represents the energy level of the chain alone, (B) represents the energy level of the bridge alone, and (C) shows the resultant energy level of the interaction between the bridge and the chain.

5.3.2. Effect of the cyclization

The effect of cyclization on the spectral position of the absorption band can be interpreted within the framework of perturbation theory (see, for example, [18]). The change in the energy of the ith molecular orbital upon cyclization may be described by the general formula:

$$\Delta\varepsilon_i = (\varepsilon_i - \varepsilon_j)^{-1} \left(\sum_n \sum_m C_{in} C_{jm} \beta_{nm} \right)^2, \qquad (4)$$

where ε_i and C_{in} are the energy and coefficients of the ith molecular orbital of the unsubstituted dye molecule; ε_j and C_{jm} are the energy and coefficients of the jth molecular orbital of the bridge; β_{nm} is the resonance integral of the bonds formed upon cyclization, which characterizes the interaction between the nth atom of the chain and the mth atom of the bridge. It is important to note that $j = 1$ because only the first MO of the bridge affects the energy position of the molecule.

Trimethylene bridge is the six-membered cycle in *PD 2338*. The central CH_2-group of this bridge is not in the plane of the molecule. Therefore, the influence of the bridge is equivalent to (or can be modeled by) the electronic effect of two methyl groups (CH_3) interacting with the π-electron system of the chain [19]. The interaction of the CH_3 group with the π-electron levels of the

chain is described in the frame of the so called "hyperconjugation" model [19]. From this model it follows that each CH_3 group has only one level (or one MO), which is placed far from both the HOMO and LUMO levels of the chain. Therefore, the influence of the bridge is relatively small, but not zero. From Eq. (4) it follows that the effect of the bridge on the energy level of the dye is proportional to the square of the coefficients C_{in} and C_{jm} and inversely proportional to the energy difference between the molecular orbitals of the dye molecule and the bridge. For PD 2338 this interaction is schematically presented in Fig. 12(b). The circles at HOMO and LUMO levels correspond to the values of the electron density distribution. As can be seen, the interaction will only be substantial between two levels of the two CH_3 groups and the HOMO level of the chain because of the non-zero values of the coefficients at the cyclization atoms (positions 1 and 2). At the LUMO level the charges are negligible. As a result, the interaction leads to a decrease in the energy difference between HOMO and LUMO levels, which leads to a red shift of the absorption band. This trend is observed experimentally.

Dimethylene bridge is the five-membered cycle in *PD 1952*. In contrast to the trimethylene bridge it is placed in the molecular plane and is characterized by an additional interaction between two rigid fixed CH_2-groups. Due to this interaction, the molecular orbital of the bridge itself is split into two levels: symmetrical (s) and asymmetrical (a), see Fig. 12(c). Analysis of Eq. (4) accounting for the signs of all coefficients shows that the interaction is substantial only between the two asymmetrical orbitals (bridge and HOMO orbital of the chain). The interaction between symmetrical orbitals of the bridge and LUMO of the chain is negligible because of nearly zero coefficients at the cyclization atoms (positions 1 and 2 of LUMO orbital). Thus such cyclization leads to a decrease in the energy difference between the HOMO and LUMO levels resulting in a red shift of the absorption band that is similar to the previous case. This trend is also observed experimentally. This information for PD 1952 is schematically presented in Fig. 12(c).

Vinylene bridge in *PD 2410* is the five-membered vinylene cycle conjugated with the main π-electron system of the polymethine chromophore. The vinylene bridge possesses its own π-electron system, thus causing the splitting of the molecular orbital of the bridge to be so large that its asymmetric level (a) becomes higher in energy than the LUMO of the chain, see Fig. 12(d). It is seen from this Figure that LUMO coefficients are negligible in the positions of cyclization (1 and 2) resulting in a negligible interaction with the orbitals of the bridge. On the contrary, the interaction between the asymmetrical orbitals of the bridge and HOMO of the chain should be substantial. Therefore, introduction of the vinylene bridge into the polymethine chromophore causes a decrease in the energy of the HOMO level and hence, leads to a blue shift of the absorption band.

5.3.3. Nature of the higher electron transitions in PD 2410

It is shown in Fig. 12(d) that the occupied level of the vinylene bridge is situated close to the HOMO level of the dye, in contrast to the remote displacement of the corresponding levels in the other dyes, substituted PD 1952 and unsubstituted PD 3428. Therefore, the $S_0 \rightarrow S_2$ and higher electron transitions may involve the interaction with these levels of the vinylene bridge. The different nature of the higher electron transitions $S_0 \rightarrow S_n$ ($n = 2, 3, \ldots$) for PD 2410 in contrast to PDs 3428 and 1952 can be illustrated by the diagrams of the electron redistribution presented in Fig. 13. It follows from Fig. 13 that the nature of the $S_0 \rightarrow S_1$ transition is the same for all dyes; there is only a small influence of the charges in the vinylene bridge as shown in Fig. 13. The nature of the second transition in PD 2410 does not coincide with the corresponding transitions in the other dyes. Instead of the usual electron transfer from the atoms in the odd position to the even position of the polymethine chain, this transition is mainly connected with electron transfer from the outer part of the chain to the central five-membered conjugated cycle. The calculations predict that a similar electron transfer will occur from the outer part of the chain to the central cycle for the $S_0 \rightarrow S_4$ transition in PD 2410, while the nature of the $S_0 \rightarrow S_3$ transition is similar to the $S_0 \rightarrow S_3$ transition in the other dyes, except for the slight decrease in the electron density at the carbon atom in the mesoposition of the chain.

Thus, introduction of the vinylene bridge with its own two levels placed near the frontier (HOMO and LUMO) levels of the main chromophore in PD 2410, is accompanied by changes in the nature of the two transitions $S_0 \rightarrow S_2$ and $S_0 \rightarrow S_4$. Orientation of these transitions is connected with electron transfer from the outer region to the center of the chain (along the polymethine chromophore), which is the same as for the $S_0 \rightarrow S_1$ transition. These changes in the nature of the electron transfer are responsible for the unusual behavior of the excitation anisotropy function for PD 2410 (Fig. 4d). All three transitions $S_0 \rightarrow S_2$, $S_0 \rightarrow S_3$ and $S_0 \rightarrow S_4$ are characterized by relatively high and approximately equal anisotropy values (about 0.3), which means nearly collinear orientation of the absorption and fluorescence transition dipole moment for all three transitions. This is in contrast to the behavior of PD 1952 in which the anisotropy values for $S_0 \rightarrow S_2$ and $S_0 \rightarrow S_4$ transitions are close to zero.

5.4. Anisotropy in ESA transitions

We have shown in Section 4.2 that in all polymethine molecules the ESA transition dipole moments (the most

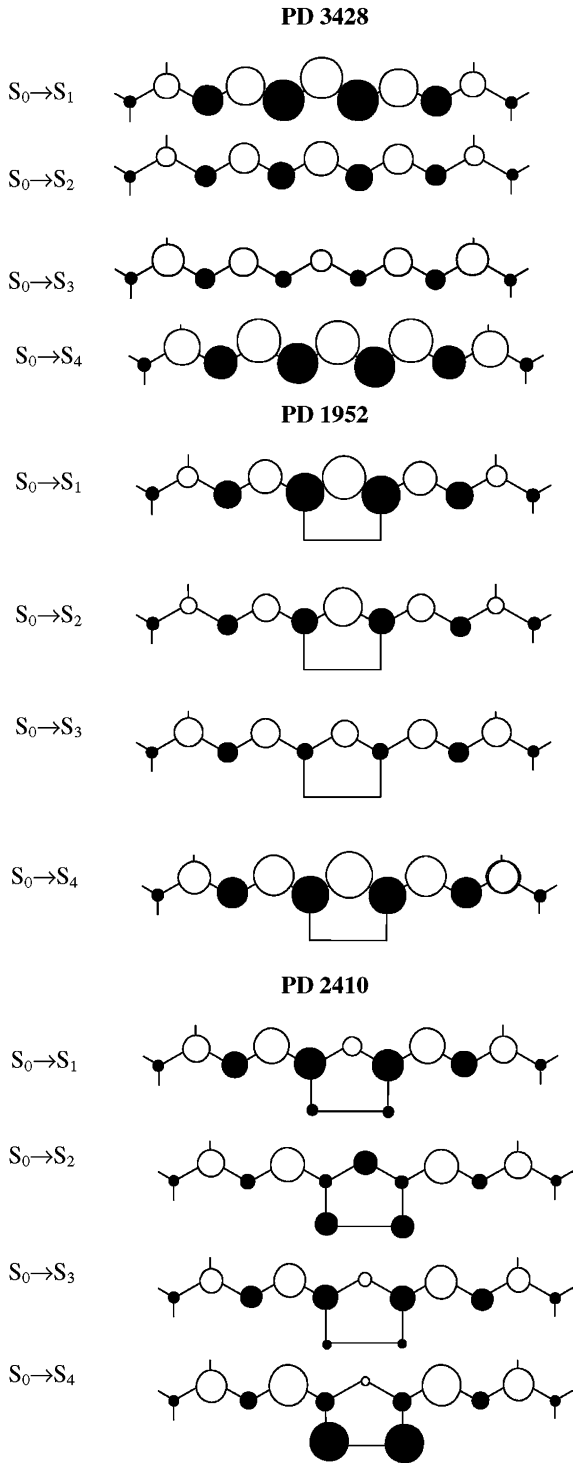

Fig. 13. Electron energy redistribution on transitions $S_0 \rightarrow S_n$ ($n = 1$–4) for PD 3428, PD 1952, and PD 2410. Dark circles correspond to an increase of electron density due to a transition, while the white circles correspond to a decrease. The diameters of the circles reflect the values of electron density change.

intense $S_1 \rightarrow S_5$ transition was used in these cases) can be used for determining the orientation of the $S_0 \rightarrow S_n$ transitions instead of the fluorescence transition dipole moment ($S_1 \rightarrow S_0$). This important result can be explained using the following three concepts. *First*, polymethine molecules are linear conjugated molecules, so the most intense absorption band occurs for the transition in which all π-electron centers are involved in the transition and the transition dipole moment is parallel to the direction of the polymethine chain (or molecular backbone), which is the $S_0 \rightarrow S_1$ transition. This well-known conclusion is based on the analysis of the linear absorption ($S_0 \rightarrow S_n$) spectra and quantum-chemical theories [12,13,17]. Our calculations show that for all the PDs studied the $S_0 \rightarrow S_1$ transition dipole moment is much larger (20–400 times) than all higher transitions ($S_0 \rightarrow S_n$, $n > 1$). *Secondly*, the most intense excited-state transitions are parallel to the polymethine chain [2,4], again due to the fact that these molecules are linear conjugated molecules. These transitions that are parallel to the polymethine chromophore are the only observable $S_1 \rightarrow S_n$ transitions. The small percentage of the population in the excited state (N_1) makes it difficult to observe weak excited-state transitions. From our calculations, the largest percentage of molecules in the excited state is 15% of the total population. All excited-state transitions that are oriented at a relatively large angle to the molecular backbone are weak and are thus unlikely to be observed. In the ground state the weak transitions ($S_0 \rightarrow S_n$, $n > 1$) are observable due to the high concentration of molecules in the ground state ($N_0 \approx N$, where N is the total population). This large difference in population between the ground and excited state ($N_0 \leqslant N_1$) is the reason why only strong excited-state transitions oriented parallel to the polymethine chromophore are observable. *Finally*, the energy level that both the ESA and fluorescence processes probe is the same relaxed S_1-state that is formed from the Franck–Condon excited state after vibrational relaxation. Our experiments, performed previously with the femtosecond nonlinear spectrometer [2], have shown that the formation of the vibrational structure of the ESA-spectrum in the visible region for typical PDs is complete in approximately 1–1.5 ps. Therefore, this time can be considered as the time of excited-state geometry optimization adapting to the new excited-state charge distribution. During this time the valence angles and bond lengths can change their initial values leading to a change in the orientation of the polymethine chromophore. This process was described in detail in Section 5.2. As a result, all excited-state molecules are aligned parallel to this new orientation of the polymethine chromophore affecting both ESA ($S_1 \rightarrow S_n$) and fluorescence ($S_1 \rightarrow S_0$) transitions.

These three reasons explain why the anisotropy of the ground to excited-state transitions in PDs can be monitored by the ESA of a probe beam instead of being monitored by the fluorescence intensity. As for molecules that are not linear and possess more than one intense ground state transition (i.e., phthalocyanines or porphy-

rins) the analysis is not so straightforward and is currently being investigated.

6. Conclusion

We have described a detailed investigation of the fluorescence and ESA anisotropy spectra for a series of polymethine molecules with different substitutions of the polymethine chromophore and different lengths of the chain. It is found that in all polymethine molecules studied the excited-state transition dipole moments can be used for determining the orientation of the $S_0 \rightarrow S_n$ transitions instead of the fluorescence transition dipole moment ($S_1 \rightarrow S_0$ transition). The two-color polarization-resolved pump–probe ESA method allows us to resolve all features in the anisotropy behavior for polymethine dyes. Therefore, we conclude that the ESA anisotropy method represents a useful approach for linear conjugated molecules like the polymethine, which can be applied to cases in which the steady-state fluorescence anisotropy measurements cannot be used, for example, in cases of nonfluorescent (or low fluorescence quantum yield) molecules, which is typical for long wavelength absorbing dyes, or for solvents with low viscosity which decrease the anisotropy value due to reorientational diffusion. We are currently investigating if this method is applicable for other types of molecules.

We have performed a detailed quantum-chemical analysis of the changes in molecular geometry and electron density distribution in the ground and excited state. It was assumed that the deformations in the molecular geometry under excitation (from Franck–Condon to relaxed), accompanied by the changes in the valence angles and bond lengths, are responsible for the anisotropy changes from the theoretical value of 0.4 to the range of values of 0.3–0.38 for the $S_0 \rightarrow S_1$ transition (depending upon the dye). This conclusion is based on the experimental results that there is no change in anisotropy value due to vibrational coupling. On the basis of quantum-chemical calculations, the effect of the polymethine chromophore cyclization with different types of bridges was explained. The conjugated vinylene bridge strongly affects the nature of the higher electron transitions leading to the unusual behavior of the excitation anisotropy function in PD 2410.

Acknowledgements

The authors gratefully acknowledge the support of the National Science Foundation (Grant No. ECS-0217932) and the Naval Air Warfare Center Joint Service Agile Program (Contract No. N00421-98-C-1327).

References

[1] J.H. Lim, O.V. Przhonska, S. Khodja, S. Yang, T.S. Ross, D.J. Hagan, E.W. Van Stryland, M.V. Bondar, Yu.L. Slominsky, Chem. Phys. 245 (1999) 79.
[2] R.A. Negres, O.V. Przhonska, D.J. Hagan, E.W. Van Stryland, M.V. Bondar, Yu.L. Slominsky, A.D. Kachkovski, IEEE J. Sel. Top. Quantum Electron. 7 (2001) 849.
[3] O.V. Przhonska, D.J. Hagan, E. Novikov, R. Lepkowicz, E.W. Van Stryland, M.V. Bondar, Yu.L. Slominsky, A.D. Kachkovski, Chem. Phys. 273 (2001) 235.
[4] R.S. Lepkowicz, O.V. Przhonska, J.M. Hales, D.J. Hagan, E.W. Van Stryland, M.V. Bondar, Yu.L. Slominsky, A.D. Kachkovski, Chem. Phys. 286 (2003) 277.
[5] M. Hamer, The Cyanine Dyes and Related Compounds, Interscience Publisher, New York, 1964 p. 790.
[6] A.I. Tolmachev, Y.u.L. Slominsky, A.A. Ischenko, New cyanine dyes absorbing in the NIR region, in: S. Daehne, U. Resh-Genger, O.S. Wolfbeis (Eds.), Near-Infrared Dyes for High Technology Applications, NATO ASI Series, vol. 52, Kluger Academic Publishers, Dordrecht, Boston, London, 1998, pp. 385–415.
[7] J.R. Lakowicz, Principles of Fluorescence Spectroscopy, second ed., Kluwer Academic/Plenum Publishers, New York, 1999 p. 698.
[8] H.E. Lessing, A. Von Jena, Chem. Phys. Lett. 59 (1978) 249.
[9] A. Penzkofer, J. Wiedmann, Opt. Commun. 35 (1980) 81.
[10] J.S. Craw, J.R. Reimers, G.B. Bacskay, A.T. Wong, N.S. Hush, Chem. Phys. 167 (1992) 77.
[11] J.S. Craw, J.R. Reimers, G.B. Bacskay, A.T. Wong, N.S. Hush, Chem. Phys. 167 (1992) 101.
[12] A.D. Kachkovski, Russ. Chem. Rev. 66 (1997) 647.
[13] S. Daehne, Science 199 (1978) 1163.
[14] J.R. Reimers, N.S. Hush, Chem. Phys. 176 (1993) 407.
[15] Yu.N. Bernatskaya, A.D. Kachkovski, Teor. Eksper. Khim. (Russian) 35 (1999) 142.
[16] A.D. Kachkovski, O.O. Zhukova, Teor. Eksper. Khim. (Russian) 37 (2001) 280.
[17] J. Fabian, R. Zahradnic, Z. Wiss, Techn. Univ. Dresden 26 (1977) 315.
[18] M.J.S. Dewar, The Molecular Orbital Theory of Organic Chemistry, McGraw-Hill, New York, 1969.
[19] A. Streitwiser, Molecular Orbital Theory for organic chemists, Wiley, New York, London, 1963.